

Ion Propulsion Plasma Interactions in the Solar Wind

Joseph Wang*

Jet Propulsion Laboratory, California Institute of Technology, Pasadena

1. Introduction

Ion propulsion will be used for the first time on an interplanetary spacecraft, the New Millennium Deep Space One (DS1), scheduled for launch in July 1998. A primary objective of New Millennium DS1 is to flight validate solar electric propulsion (SEP) for interplanetary missions. The cruise phase of the mission will characterize the life and performance of a 30 cm xenon ion thruster and determine how its operation may affect spacecraft payloads and critical subsystems.

Effects introduced by the operation of the ion thruster have long raised both technology and science concerns. The technology concerns include plume backflow contamination and spacecraft interactions with the induced plasma environment. Backflow contamination can lead to effluent deposition that can affect thermal control surfaces, optical sensors, solar arrays, science instrumentation, and communications. The induced plasma environment will modify spacecraft charging characteristics, and can lead to plasma interactions with the solar array. The science concerns relate to plasma measurements. The plume will modify the properties of the solar wind flowing around the spacecraft and may contaminate measurements of the ambient plasma and magnetic fields. As ion thrusters are designed to operate for long periods of time, these effects need to be carefully assessed.

This paper focuses on the plasma physics issues related to ion propulsion. We present an overview of our current understanding of ion thruster plume induced plasma interactions and discuss the planned investigations of such interactions from the DS1 mission. In section 2, we briefly discuss the properties of the plasmas emitted from the NSTAR (NASA Solar-Electric Propulsion Technology Application Readiness) thruster to be used on DS1 and the resulting near-field plume-spacecraft interactions. This establishes the properties

of the ion thruster plume in the absence of an ambient environment. In section 3, we include the solar wind environment and discuss plume induced plasma interactions in the solar wind. In particular, we consider interactions far away from the thruster exit and study whether any plume-solar wind coupling may occur via collisionless mechanisms. Due to the complexity of the problem, the difficulty of matching space conditions in a laboratory, and the lack of opportunities to flight test ion thrusters, computer particle simulations have recently become the best means to study ion thruster induced interactions. Hence, the discussions in section 2 and section 3 will be limited to predictions based on particle simulations. In section 4, we discuss the planned DS1 plasma physics investigations on ion propulsion, which include a correlated data analysis and modeling effort. Section 5 contains a summary and conclusions.

2. Ion Thruster Plume

We first review ion thruster plume interactions near the spacecraft. The interactions induced by ion thruster plumes have been studied for some time. Recently, *Samanta Roy et al.*[1996a,1996b] used hybrid PIC simulations to model the far-downstream region and study charge exchange ion backflow. *Wang and Brophy*[1995] and *Wang et al.*[1996] developed full particle and hybrid PIC-MCC models of single and multiple thruster plumes and carried out 3-D particle simulations of ion thruster plume environments using parameters similar to those of the NSTAR ion thruster. *Katz et al.*[1997] studied electric potentials in the NSTAR charge exchange plume predicted using a barometric law and a finite current parmetric law for electron densities.

The Ion Thruster Plasma

In ion thrusters, propellant ions are accelerated electrostatically by a system of grids to form a high velocity beam; neutralizing electrons are emitted from the neutralizer in conjunction with the beam ions. Thus the ion thruster plume is composed of propellant efflux (including beam ions, neutralizing electrons, and neutrals

*Senior Member Technical Staff, Advanced Propulsion Technology Group; Member of the Deep Space One Mission Science Team; Member AIAA

that escape through the ion optics and from the neutralizer), nonpropellant efflux (material sputtered from thruster components and the neutralizer), and a low-energy plasma generated through charge-exchange collisions between energetic ions and the neutrals within the plume.

The 30 cm xenon NSTAR thruster to be used on DS1 has an input power range of 600 to 2500 W. Under typical operating conditions, the beam current is about 1.76 A; and the exit beam velocity is about 3.5×10^6 cm/s (beam ion kinetic energy about 1 keV); Near the thruster exit, the temperature of beam ions is about 0.04 eV (~ 500 K), and the temperature of the neutralizing electrons is in the range of 1–5 eV. From these parameters, the average beam ion current at the thruster exit is $J_{bi0} = I/\pi r_T^2 \simeq 24.9 \text{ A/m}^2$ and the average beam ion density at the thruster exit $n_{b0} = J_{bi0}/ev_{bi} \simeq 4.4 \times 10^9 \text{ cm}^{-3}$. The propellant ions form a divergent beam with a divergence half angle about 15 to 20° due to the curvature of the thruster exit surface. The radial beam current density profile may be assumed to follow a Gaussian distribution, although the actual distribution may be more peaked at the center.

The propellant that remains unionized flows out of the thruster exit in free molecular flow at thermal speeds corresponding to the thruster wall temperature (~ 500 K). The density of the neutral plume near the thruster exit is about 10^{12} cm^{-3} and remains quasi-steady due to the low charge-exchange collision rate. For $v_{bi} \simeq 3.5 \times 10^4$ m/s, we find that the charge-exchange collision cross section $\sigma_{ceex} \simeq 3.5 \times 10^{-15} \text{ cm}^2$. Hence, at the thruster exit, we find the charge-exchange ion production rate $\frac{dn_{ceex}}{dt} \simeq 2.4 \times 10^{13} \text{ cm}^{-3} \text{ s}^{-1}$. In addition to these propellant and charge-exchange ions a very small amount of neutrals may also undergo photoionization or charge-exchange ionization in the solar wind.

Near-Field Plume-Spacecraft Interactions

As the solar wind density is about 1 cm^{-3} , it is appropriate to neglect the solar wind plasma as a first approximation. Under the solar wind magnetic field, the gyro-radius for the beam ions and the charge exchange ions is much larger than the size of the spacecraft, Hence, the solar wind magnetic field can also be neglected for the near-field region. Thus, the interaction is electrostatic.

During normal ion thruster operation, electron emission keeps the exhaust plume quasineutral and prevents the spacecraft from charging up significantly. Typically the spacecraft potential $\Phi_{s/c}$ is much lower than that of the beam ion kinetic energy, $|e\Phi_{s/c}| \ll KE_{bi0}$. In the absence of an external electromagnetic field, the beam

ions follow nearly line-of-sight trajectories because the electric field within the plume is too small to perturb their motion. Hence, the core region of the ion beam will keep its coherent structure. The electrons are much more mobile than ions, so the center of the plume has a positive potential. This potential causes the slowly moving charge-exchange ions to move transversely out of the plume.

Wang *et al.* [1995,1996] have developed a fully three-dimensional hybrid particle-in-cell Monte Carlo collision model of the near-field plume environment. In this model, the ions are represented by individual superparticles and the electrons are assumed to have a fluid response in which the density is approximated by the barometric law. A typical simulation setup is shown in Fig.1a. The spacecraft is modeled as a 3-dimensional box structure with a conducting surface and a surface potential Φ_w relative to the ambient. At each time step, the propellant ions are injected into the simulation domain from the thruster exit to form a beam with a Gaussian density distribution in the radial direction and a divergent half angle of about 15°. The neutral plume is treated as a steady state background produced by a free molecular flow. A Monte Carlo representation of particle collisions is utilized to model the charge-exchange collision between the beam ions and the neutral background. The charge-exchange ions are generated according to

$$\frac{dn_{ceex}}{dt} = n_{bi}n_n v_{bi} \sigma_{ceex}(v_{bi}) \quad (1)$$

based on the beam ion and neutral density profile. The trajectory of each charged particle is integrated from

$$\frac{dm\vec{V}}{dt} = \vec{F} = q(\vec{E} + \vec{V} \times \frac{\vec{B}}{c}), \quad \frac{d\vec{x}}{dt} = \vec{V} \quad (2)$$

using a standard leapfrog scheme, and the self-consistent electric field is obtained from the Poisson's equation

$$\nabla^2 \Phi = -4\pi\rho \quad (3)$$

Some typical simulation results are shown in Fig. 2. For this simulation, the spacecraft is taken to be a cubic box with dimension $1m \times 1m \times 1m$. The spacecraft is located at $2 \leq x \leq 16$, $15 \leq y \leq 29$, and $15 \leq z \leq 29$. The thruster exit center is located at $x = 18$, $y = 22$, and $z = 22$. The thrust direction is in the x direction. The grid resolution is taken to be $d_{cell} \simeq 5.2 \text{ cm}$. The spacecraft potential is taken to be $\Phi_{s/c}/T_e \simeq -3$. Fig.2 shows the contours of potential and the total ion density and the vectors of the charge-exchange ion current density on a xy plane cutting through the spacecraft and

thruster center. We find that the outflow of the charge-exchange ions forms a wing-shaped structure. Once outside the plume, the charge-exchange ions come under the influence of the potential of the spacecraft sheath. As the spacecraft potential is typically negative, these ions will therefore be drawn back to the spacecraft.

An uncertainty in most hybrid PIC plume simulations so far is the use of the barometric law approximation for the electron density. Recently, *Katz et al.*[1997] studied the validity of this approximation. They found that the barometric law provides a good approximation when the ambient plasma density is high or the electron current is small. However, when the ambient density is very small such as that for the interplanetary plasma environment, the barometric law would lead to predictions of an unrealistically high potential within the plume [*Katz et al.*,1997; *Gardner et al.*, 1997]. A new “finite current barometric” law was thus developed. Currently, full particle simulations using a 3-D full particle PIC code *Wang and Lai*[1997] are being performed to resolve the electron characteristics near the thruster exit theoretically.

3. Plume Interactions in the Solar Wind

For an interplanetary spacecraft such as the DS-1, the ion thruster operates in the solar wind, which is a tenuous, relatively hot plasma with a high flow speed and a frozen-in magnetic field. The presence of the solar wind environment may induce complex plume-solar wind interactions. Almost all studies on ion thruster plume interactions so far have concentrated on charge-exchange ion interactions near the spacecraft while few addressed other aspects of plume interactions. A preliminary study of plume interactions in the solar wind was recently presented by *Wang et al.*[1997].

It is instructive to first review theoretical studies of solar wind interactions with newborn ions related to comets and collisionless shocks. Generally speaking there are three mechanisms by which newborn ions may interact with the solar wind plasma and magnetic field. The first is particle/particle Coulomb collisions which is relatively weak due to the low density of the solar wind. The second process is cyclotron pickup, in which the motional electric field of the solar wind accelerates the newborn ion which then gyrates around a magnetic field line. The third mechanism is scattering of the ions by wave/particle interactions. The consequences of the collisionless second and third mechanism are studied in numerous papers for homogeneous plasmas. For instance, *Wu and Davidson*[1972] are among the first to point out that the newly ionized particles

in the solar wind can result in collective instabilities that generate large-amplitude electromagnetic waves. *Gary et al.*[1984,1986] presented linear theories and 1-dimensional simulations of electromagnetic instabilities driven by a cool ion beam parallel or anti-parallel to the solar wind magnetic field. *Omidi and Winske*[1987] performed hybrid simulations on the kinetic processes associated with solar wind mass loading due to pickup of cometary ions and the formation of cometary bow shocks. A review of electromagnetic ion/ion instabilities in space plasmas is found in [*Gary*,1991]. In principle, kinetic couplings between the solar wind and newborn ions could also occur to an ion thruster plume in the solar wind. Hence, we next consider ion thruster plume interactions in the solar wind.

The Solar Wind Plasma

The solar wind is a tenuous, relatively hot plasma which flows radially outward from the sun. Since the magnetic field is approximately “frozen” in the conducting solar wind, the solar magnetic field is convected out into space by the solar wind. The expansion of the solar wind plasma across the interplanetary magnetic field also induces a motional electric field in the reference frame at rest with respect to the Sun, $\vec{E}_o = -\vec{v}_{sw} \times \vec{B}_o$. In the reference frame of the solar wind, $\vec{E}_o \simeq 0$. Typical values of solar wind parameters are: solar wind density $0.5 \text{ cm}^{-3} < n_{sw} < 10 \text{ cm}^{-3}$, solar wind flow speed $300 \text{ km/s} < v_{sw} < 500 \text{ km/s}$, solar wind ion temperature $2 \text{ eV} < T_i < 20 \text{ eV}$, and solar wind magnetic field magnitude $1.0 \text{ nT} < B_o < 20 \text{ nT}$. The angle between the solar wind flow velocity \vec{v}_{sw} and the interplanetary magnetic field \vec{B}_o , α , can vary from 0° to 90° and is a crucial parameter in much of the physics involved.

Plume Interactions in the Solar Wind

The global scale plume-solar wind interaction is illustrated in Fig.1b. In the vicinity of the thruster, since the thruster plume will dominate the spacecraft environment due to their much higher density, the plume will blow a cavity in the solar wind modify the solar wind as it flows past the plume region. Far away from the thruster where the plume density has decreased to a level that the solar wind plasma and fields can penetrate the plume, the plume ions may couple with the solar wind through collective plasma effects similar to new born ion-solar wind interactions of comets and collisionless shocks.

The plume-solar wind interaction has very different characteristics from the near-field plume-spacecraft interaction discussed in section 2. In particular, while the plume-spacecraft interaction is electrostatic in nature, the couplings between the plume ion and the solar

wind is electromagnetic in nature. Hence, our approach is based on electromagnetic hybrid particle simulation [Winske and Omid, 1993]. Since the interactions only concern the ion dynamics, the basic assumptions in our approach are a) the electrons are a massless fluid $m_e = 0$ while the ions are treated as test particles, and b) the displacement current $\frac{\partial \vec{E}}{\partial t}$ can be neglected in Ampere's law (for low frequency waves). Since we are concerned with a quasineutral plasma in a global region, quasineutrality is assumed. Therefore, the governing equations are

1) Quasineutrality:

$$n_e = n_i \quad (4)$$

2) Maxwell's equations in the low frequency approximation:

$$\nabla \times \vec{B} = \frac{4\pi}{c} \vec{J} \quad (5)$$

$$\nabla \times \vec{E} = \frac{\partial \vec{B}}{\partial t} - \frac{1}{c} \quad (6)$$

$$\nabla \cdot \vec{B} = 0 \quad (7)$$

3) The electron fluid equation in the limit of $m_e = 0$:

$$\frac{\partial n_e m_e \vec{V}_e}{\partial t} = 0 = -en_e(\vec{E} + \vec{V} \times \frac{\vec{B}}{c}) - \nabla \cdot \mathbf{P}_e + en_e \mathbf{R} \cdot \vec{J} \quad (8)$$

where the electron pressure tensor is given by:

$$\mathbf{P}_e = n_e T_e \mathbf{I} \quad (9)$$

and the resistivity tensor $\mathbf{R} = \eta \mathbf{I}$ describes short wavelength, high frequency wave-particle interactions not explicitly included in the hybrid model; and

4) Dynamic equation for individual ion particles

$$m_i \frac{d\vec{v}_i}{dt} = \vec{F} = q(\vec{E} + \vec{v}_i \times \frac{\vec{B}}{c}) - q\eta \vec{J}, \quad \frac{d\vec{x}_i}{dt} = \vec{v}_i \quad (10)$$

Far-Field Plume-Solar Wind Coupling

In this paper, we shall only consider the far-field region where the plume has become sufficiently rarefied so that the solar wind can penetrate into the plume. Solar wind-plume interactions in the vicinity of the thruster is still a subject of ongoing research. The distance from the "far field" region to thruster exit, L , may be estimated as follows:

The beam ion current at a distance L from the thruster is given by

$$I = n(\pi r^2)v = n_0(\pi r_0^2)v$$

where n_0 and r_0 are the beam ion density and beam cross section radius at thruster exit, respectively.

Hence, the beam density at a distance L from the thruster exit is approximately

$$\frac{n}{n_0} \sim \left(\frac{r_0}{r}\right)^2$$

and the distance L is given by $L \sim r/\tan(15^\circ)$ (for a 15° divergence angle). Therefore, for the beam ion density to decrease from $n_0 \sim 10^9 \text{ cm}^{-3}$ at thruster exit to approximately the level of the solar wind density $n \sim 10 \text{ cm}^{-3}$, we find the distance to be $L \sim 5 \text{ km}$.

We note that the far-field plume-solar interactions occur at a length scale much larger than the spacecraft size. For convenience, we choose a reference frame moving with the solar wind. Hence the solar wind sees a plume moving with a relative velocity $-\vec{v}_{sw} + \vec{v}_{plume}$. As \vec{v}_{sw} is much larger than the beam ion velocity, the relative drift velocity between the solar wind and the plume is dominated by the solar wind flow speed. Hence, we do not need to distinguish between the beam ions and the charge-exchange ions. Since our emphasis here is on the consequences of the collisionless process, we shall consider a $2\frac{1}{2}$ -dimensional (2 spatial components, three velocity and field components), homogeneous model shown in Fig.1b. We take the relative velocity $\vec{v}_{dx} = -\vec{v}_{sw} + \vec{v}_{plume}$ along the x direction, and the angle between x and the solar wind magnetic field to be α . Initially, the solar wind protons follow a Maxwellian distribution with a temperature of 10 eV and the plume ions follow a drifting Maxwellian distribution centered around \vec{v}_{dx} with a temperature of 0.04 eV.

In Figs. 3 and 4., we present some typical electromagnetic hybrid simulation results. we consider two flow conditions, the parallel flow ($\alpha = 0^\circ$) and the perpendicular flow ($\alpha = 90^\circ$) conditions. We take the plume to solar wind density ratio to be $n_X/n_{sw} \sim 100$. Due to computational limitations, an artificial proton mass of $m_p/m_X = 16^{-1}$ is used. This compresses the relative plume ion and solar wind proton gyroperiods but does not affect the qualitative picture of the physics. In the solar wind reference frame, the relative plume velocity normalized by the Alfvén speed for the plume ions, $v_{AX} = B_0/\sqrt{4\pi n_X m_X}$, is $v_{dx}/v_{AX} \simeq 63.2$.

The velocity distributions for the plume ions and the solar wind protons for the $\alpha = 0^\circ$ case are shown in Fig. 3. The distribution functions are shown for $t\Omega_X = 0, 8, 16, 24,$ and 48 , where Ω_X is the gyrofrequency of the plume ions under the solar wind magnetic field. At the early stage of the interaction ($t\Omega_X \leq 8$), the velocity distributions for the plume ion show little change. However, the distribution functions for the solar wind protons have changed from an isotropic Maxwellian distribution to a drifting Maxwellian with a drifting speed

about $0.16v_{dX}$ along the x direction. This indicates that the solar wind protons are partially "picked up" by the plume. At the later stage of the interaction ($t\Omega_x > 16$), the plume ions start to lose their drifting speed and thermalize. At $t\Omega_x \geq 48$, we find that the plume ions have completely thermalized into a isotropic distribution. In other words, in the reference frame of the sun, the plume ions are swept away by the solar wind as a warm cloud. Hence, the plume has lost its original properties

The velocity distribution functions for the $\alpha = 90^\circ$ case are shown in Fig. 4. The plume ions behave similarly to that for the $\alpha = 0^\circ$ case, although the thermalization starts a little later. The solar wind protons settle to a drifting distribution with a drifting speed about $0.19v_{dX}$ during the first stage. During the second stage, the relaxation process is slower in the direction parallel to \vec{B}_0 .

To understand these results, we also analyzed the time history of the plume ion energies associated with the three velocity components and the magnetic wave energy density in the system ($(\delta B/B_0)^2$). For the $\alpha = 0^\circ$ case, we find that the magnetic wave energy starts to grow exponentially at $t\Omega_x \sim 15$, indicating an electromagnetic instability is excited. As the instability grows, wave-particle interactions drive the system toward isotropy and reduces the amount of free energy available for wave growth. Hence, the growth of wave energy is accompanied by a decrease of v_x and increases in v_y and v_z . The wave energy saturates at an almost constant level at $t\Omega_x \simeq 40$. For the $\alpha = 90^\circ$ case, the time histories have similar characteristics. However, the magnetic field fluctuations is only about 40% of that for $\alpha = 0^\circ$. This indicates that the instability is weaker in the $\alpha = 90^\circ$ case.

The physics of the collisionless plume ion-solar wind coupling can be summarized as follows. Under the perpendicular flow condition, $\alpha \sim 90^\circ$, cyclotron pickup leads to a ring-shaped newborn ion velocity distribution. Under the parallel flow condition, $\alpha \sim 0^\circ$, there are no magnetic forces on the newborn ions and the resulting distribution is a beam moving along the background magnetic field relative to the solar wind distribution. If α has an intermediate value, the newborn ions assume a ring-beam distribution. These non-Maxwellian distributions represent a strong source of free energy relative to the solar wind ion velocity distribution, and can excite a variety of instabilities which lead to enhanced fluctuations which, in turn, scatter the plume ions toward isotropization[Gary,1991].

We note that the analysis presented here only addresses the possibility and the mechanisms of solar

wind-plume interactions but does not attempt to quantify the effects of far-field interactions on the near-field environment. We only considered interactions in the far-field and assumed that the solar wind has penetrated into the plume. The homogeneous model also does not address the effects of finite plume size which inhibits growth of the electromagnetic instabilities. These issues will be addressed in our future work, which will extend this study to 3-D hybrid electromagnetic simulations to resolve plume-solar wind coupling in a global interaction region.

4. Ion Propulsion Investigations from DS1

As part of the DS1 science investigation, a joint team from JPL and Los Alamos National Lab will perform plasma physics investigations on ion propulsion and cometary ion interactions. This section briefly discusses our planned investigations related to ion propulsion plasma interactions.

DS1 carries two science instrument packages*, a Miniature Integrated Camera and Spectrometer (MICAS) and a Plasma Experiment for Planetary Exploration (PEPÉ), and an Ion propulsion Diagnostics Subsystem (IDS). The main objective of PEPÉ (P.I.: D. Young, Southwest Research Institute) is to study solar wind plasma physics, cometary plasma processes, and asteroid environments. In addition, PEPÉ can contribute to the evaluation of ion thruster induced environments. PEPÉ will perform an electrostatic energy and three-dimensional angular analysis of electron (3 eV - 30 keV) and ion (3 eV/q - 30 keV/q) distribution functions, and in addition will provide high-resolution ion composition information. The main objective of IDS (Manager: D. Brinza, JPL), which is located near the ion thruster, is to study the environment and contamination induced by the ion thruster. The IDS will have several components, including 1) quartz crystal microbalance, 2) calorimeter, 3) retarding potential analyzer (RPA) (Ion Voltage: 0 to +200 Vdc; Ion Current: 1nA to 200A), 4) Langmuir probe (LP) (Probe Bias: -14 to +14 Vdc; Current: -1 to +1 mA), 5) flux gate magnetometer (0 to 100 Hz) 6) search coil magnetometer (10 Hz to 50 kHz), and 7) plasma wave spectrometer (10 Hz to 10 MHz).

Our planned investigations will include a correlated data analysis, modeling, and comparison of modeling results with data. The analysis will address data from simultaneous PEPÉ and IDS measurement. Since these

*NASA New Millennium Deep Space One Mission information package

instruments make only single point measurements, modeling based on multi-dimensional computer particle simulations is necessary to provide a more complete description of the physics.

The ion propulsion related investigation is further divided into two parts. Our first investigation concerns the near-field plume spacecraft interactions discussed in section 2. The interaction in the near-spacecraft region is driven by the low energy charge-exchange ions responding to the local electrostatic potential. Observations for this investigation will be mostly conducted during the performance acceptance test (when the ion thruster will be operating at 6 thrust levels for about an hour at each level) and during nominal thruster operation of the cruise phase. Using the PEPE, RPA and LP data, we will analyze the velocity distribution and density of the plume ions and determine the correlation of the xenon ion density and distribution between the two extreme measurement points of PEPE and IDS. We will analyze the CEX ion flux, electron temperature, and plume potential. We will determine whether the electrons follow the Maxwellian distribution. In addition, two sets of simulations are planned to assist data analysis. The first one is to use a 3-D full particle electrostatic PIC code to study electron characteristics, deriving an effective electron temperature and comparing the results against the Langmuir probe observations. These results will give us a much better understanding of the electron characteristics in the plume and spacecraft potentials. The second one is to use a 3-D hybrid electrostatic PIC with Monte Carlo collision code to simulate the electric field and the charge-exchange ion distributions near the spacecraft as a function of solar wind parameters and thruster levels, permitting us to predict expected IDS and PEPE measurements for these quantities.

Our second investigation concerns plume-solar wind interactions discussed in section 3. This includes modifications of the solar wind by the plume in the vicinity of the thruster and far-field plume-solar wind couplings. The thrust direction is typically perpendicular to the solar wind flow direction during normal thruster operation. For this investigation, we will request that the thrust vector be pointed in several off-nominal thrust directions for short periods firings to maximize the chance of observing far-field interactions. For instance, the thrust vector may be pointed with angles between the thrust direction and the solar wind flow direction of 180, 165, 135, 45, and 0 degrees (or similar angular coverage). The most desirable observation scenario is to point the thruster vector in the direction anti-parallel to the local solar wind flow direction (angle=180 degree). We will analyze the PEPE, RPA, LP and flux gate magnetometer data for plume ion and solar wind proton

velocity distribution, charge-exchange ion flux, electron temperature, plume potential, and low frequency magnetic field fluctuations under different solar wind conditions. Another two sets of simulations will be performed to assist the data analysis. These simulations are based on the hybrid electromagnetic code discussed in section 3. The first one will be macroscopic hybrid simulations of the solar wind flow past the dense plume. This will help us to understand how the plume modifies the local solar wind properties and determine whether the plume will produce a "cavity" or shock waves in the solar wind. The second one will be local hybrid simulations at different locations to identify whether and where kinetic plume ion-solar wind coupling may occur. The ion thruster plumes obtained from the near-field simulations will provide input for the plume distribution in these simulations.

5. Summary

In conclusion, ion thruster can generate a complex set of plasma interactions. In the near-field region of the spacecraft, the interaction is driven by the low energy charge-exchange ions responding to the electrostatic potential. The presence of the solar wind environment may induce complex plume-solar wind interactions. In the vicinity of the thruster, since the thruster plume will dominate the spacecraft environment due to their much higher density, the main effect of the plume is simply to modify the solar wind as it flows past the plume region. However, far away from the thruster where the plume density has decreased to a level that the solar wind plasma and fields can penetrate the plume, the plume ions may couple with the solar wind through collective plasma effects. This is because both the low energy charge-exchange ions and the energetic beam ions constitute a free energy source, which may drive one of several electromagnetic instabilities. The instabilities can generate enhanced magnetic field fluctuations, leading to significant particle scattering. This wave particle scattering will modify the properties of both the solar wind and the plume, and may scatter the beam ions and charge-exchange ions into an isotropic distribution in the solar wind reference frame. This raises the possibility that far-field interactions may affect the plasma environment in the vicinity of the spacecraft. Other than electron characteristics near thruster exit, the plasma physics underlying the near field interaction is fairly well understood now. On the other hand, the physics underlying plume-solar wind interactions is still poorly understood. A comprehensive investigation of ion propulsion induced plasma interactions will be performed by the upcoming DS1 mission.

Acknowledgement

I would like to thank S. P. Gary of Los Alamos National Lab, P. Liewer, D. Brinza, and B. Goldstein of JPL, and W-H. Ip of Max-Plank-Institut Aeronomie for many useful discussions. This work was carried out by the Jet Propulsion Laboratory, California Institute of Technology under a contract with NASA. Access to the Cray supercomputers used in this study was provided by funding from NASA Offices of Mission to Planet Earth, Aeronautics, and Space Science.

References

- [1] B. Gardner et al., Predictions of NSTAR charge-exchange ions and contamination backflow, *IEPC Pap. 97-043*, 1997.
- [2] S.P. Gary, C. Smith, M. Lee, M. Goldstein, D. Forslund, Electromagnetic ion beam instabilities, *Phys. Fluids*, 28, 1984, pp438
- [3] S.P. Gary, C. Madland, D. Schriver, and D. Winske, Computer simulations of electromagnetic cool ion beam instabilities, *J. Geophys. Res.*, 91(A4), 1986, pp4188.
- [4] S.P. Gary, Electromagnetic ion/ion instabilities and their consequences in space plasmas: a review, *Space Sci. Reviews*, 56, 1991, pp373.
- [5] I. Katz, V. Davis, and J. Wang, Electrical potentials in the NSTAR charge-exchange plume, *IEPC Pap. 97-042*, 1997.
- [6] Omidi and Winske, A kinetic study of solar wind mass loading and cometary bow shocks *J. Geophys. Res.*, 92(A12), 1987, pp13409.
- [7] R. Samanta Roy, D. Hastings, and N. Gatsonis, Ion-thruster modeling for backflow contamination, *J. Spacecraft Rockets*, 33(4), 1996a, pp525.
- [8] R. Samanta Roy, D. Hastings, and N. Gatsonis, Numerical study of spacecraft contamination and interactions by ion-thruster effluents, *J. Spacecraft Rockets*, 33(4), 1996b, pp535.
- [9] J. Wang and J. Brophy, 3-D Monte-Carlo particle-in-cell simulations of ion thruster plasma interactions, *AIAA Pap. 95-2826*, 1995.
- [10] J. Wang, J. Brophy, and D. Binza, 3-D simulations of NSTAR ion thruster plasma environment, *AIAA Pap. 96-3202*, 1996.
- [11] J. Wang, J. Brophy, and D. Binza, A global analysis of ion thruster plume interactions for interplanetary spacecraft, *AIAA Pap. 97-3194*, 1997.
- [12] J. Wang and S. Lai, Virtual anode in ion beam emissions in space: numerical simulations, *J. Spacecraft Rockets*, 1997 (in press).
- [13] D. Winske and N. Omidi, Hybrid codes, methods and applications, in *Computer Space Plasma Physics: Simulation Techniques and Software*, edited by H. Matsumoto and Y. Omura, Tokyo, 1993.
- [14] C. Wu and R. Davidson, Electromagnetic instabilities produced by neutral-particle ionization in interplanetary Space, *J. Geophys. Res.*, 77(28), 1972, pp5399.

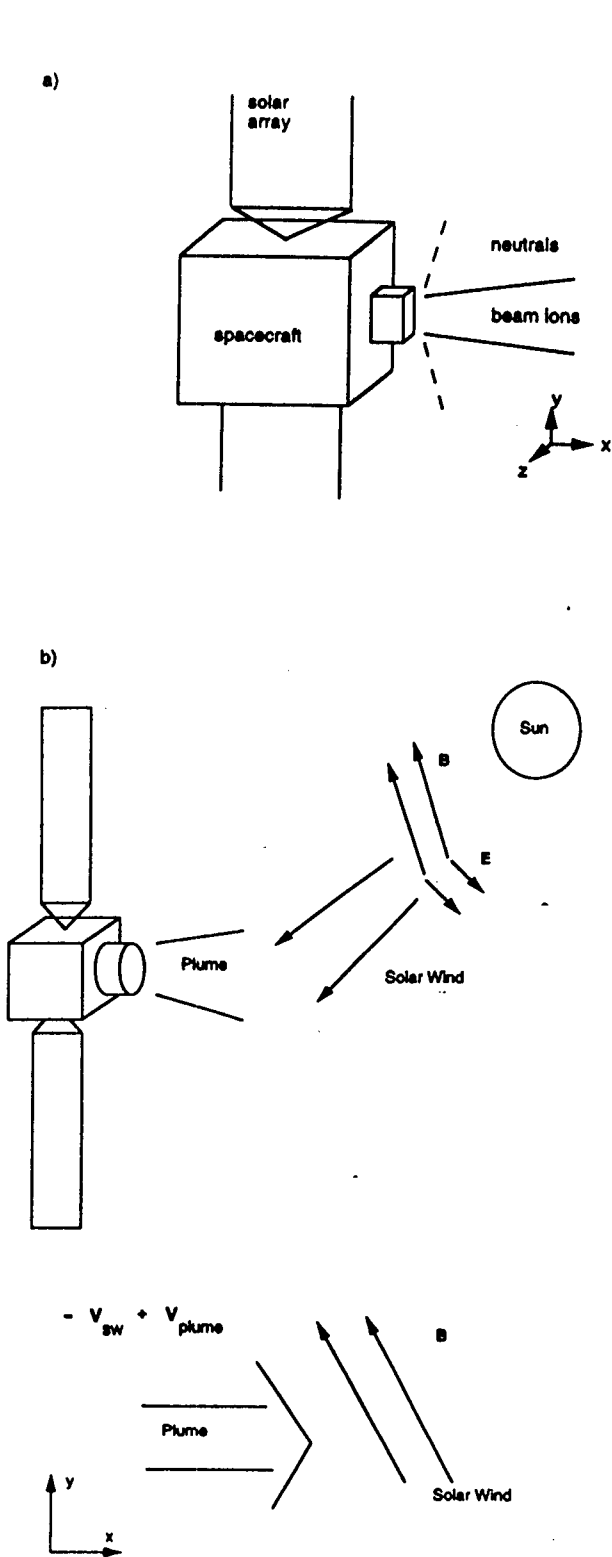


Figure 1: Model setup. a) Near-field interaction model. b) Far-field interaction model.

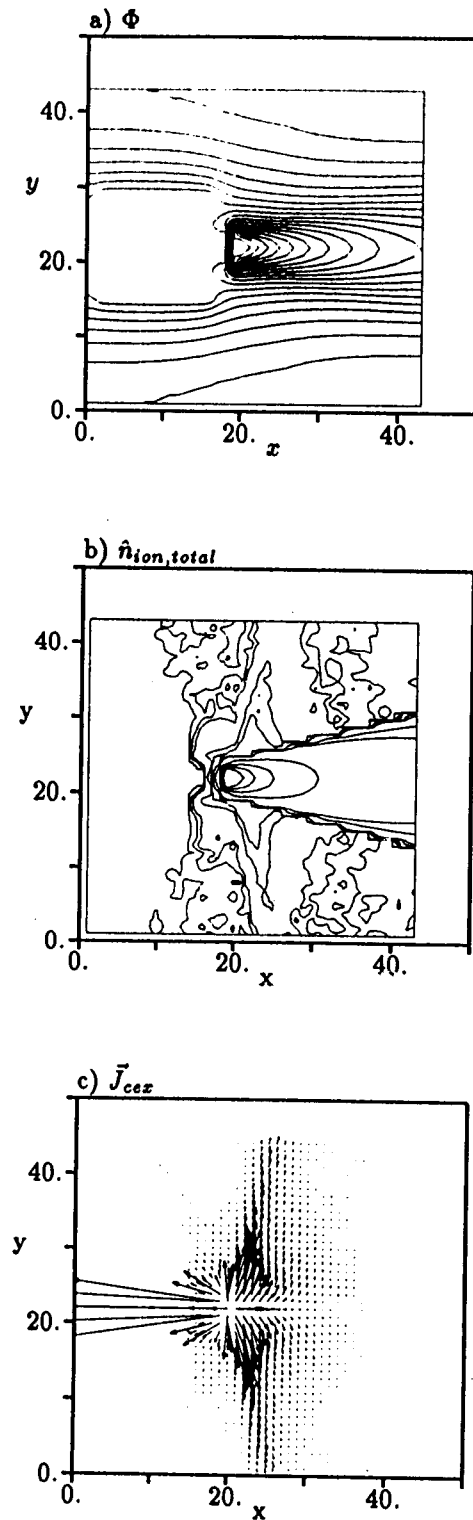


Figure 2: Plasma plume on a xy plane cutting through the center of thruster and spacecraft. a) Potential contours. b) Total ion density contours (contour level: $n_{ion}/n_{bi0} = 10^{-4}, 5 \times 10^{-4}, 10^{-3}, 5 \times 10^{-3}, 10^{-2}, 5 \times 10^{-2}, 0.1, 0.5, 1., 1.5$). c) Charge-exchange ion current vectors \vec{J}_{cex} .

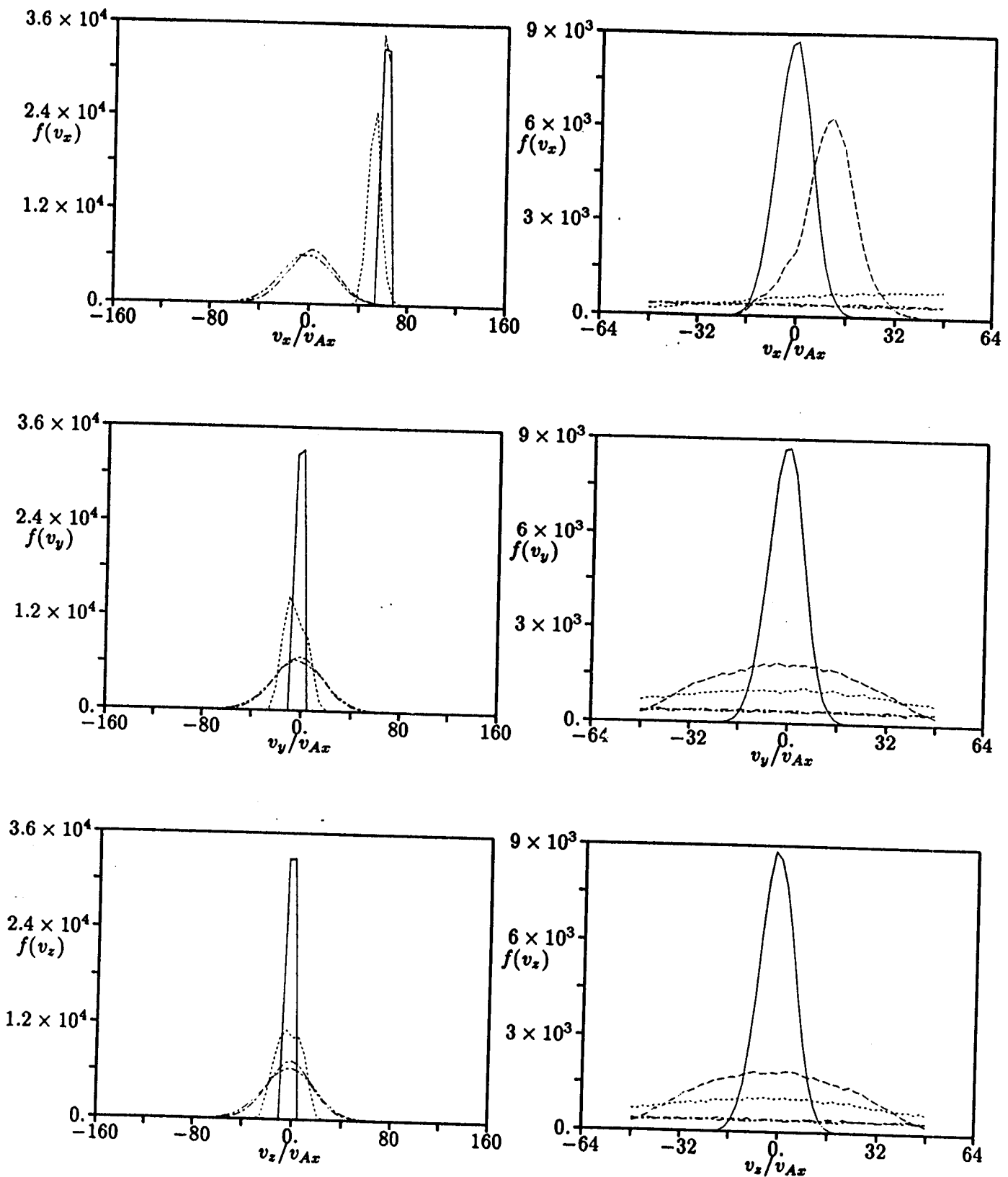


Figure 3: Plume ion velocity distributions (left column) and solar wind proton velocity distributions (right column) for the $\alpha = 0^\circ$ case. The distributions are plotted at $\Omega t = 0$ (solid), 8 (dashed), 16 (dotted), 24 (dot-dashed), and 48 (dot-dot-dashed).

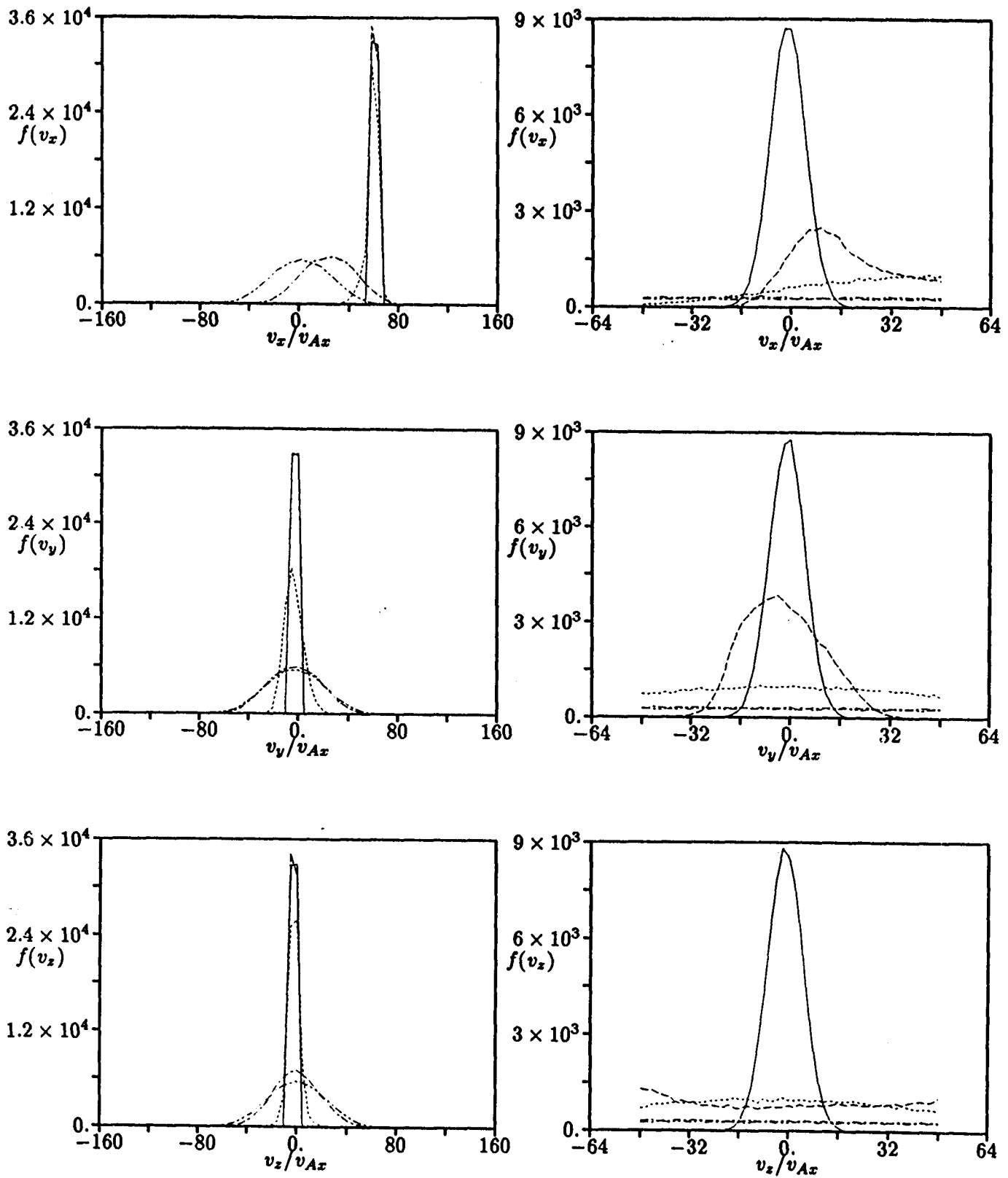


Figure 4: Plume ion velocity distributions (left column) and solar wind proton velocity distributions (right column) for the $\alpha = 90^\circ$ case. The distributions are plotted at $\Omega_{xt} = 0$ (solid), 8 (dashed), 16 (dotted), 24 (dot-dashed), and 48 (dot-dot-dashed).